

Superluminescent diodes based on asymmetric double-quantum-well heterostructures

E.V. Andreeva, S.N. Il'chenko, M.A. Ladugin, A.A. Marmalyuk, K.M. Pankratov, V.R. Shidlovskii, S.D. Yakubovich

Abstract. The power and spectral characteristics of near-IR superluminescent diodes (SLDs) based on asymmetric double-quantum-well GaAs/InGaAs heterostructures are studied experimentally. It is shown that, varying the active layer composition and the spatial-single-mode active channel length of these SLDs, it is possible to widely change the achievable output optical power and the spectral width of the symmetric bell-shaped spectrum. The studied SLDs have a lower coherence function pedestal, a weaker dependence of the spectral width on the injection current, and a higher polarisation degree than the widely spread SLDs based on single-quantum-well heterostructures with the same spectral widths.

Keywords: superluminescent diode, asymmetric double-quantum-well heterostructure.

1. Introduction

The first near-IR (800–900 nm) superluminescent diodes (SLDs) that have found practical application were based on (GaAl)As heterostructures. At present, these diodes are rather widely used as sources of high-brightness weakly coherent light in scientific studies and application fields [optical sensors of various physical characteristics, optical coherence tomography (OCT), optical metrology, etc.]. As a rule, the used SLDs have a transverse-single-mode active channel several micrometres wide, which, in particular, makes it possible to fabricate miniature single-mode fibre-coupled light-emitting modules. Apart from the output optical power, key parameters for most applications are the shape and width of the spectrum, which determine its coherence function. In particular, OCT systems (Fourier domain OCT) require a broad, approximately Gaussian spectrum. The former provides small coherence length $L_c \approx \lambda^2/\Delta\lambda$ (λ is the centre wavelength and $\Delta\lambda$ is the spectral halfwidth) and, correspondingly, a narrow central peak of the coherence function and a high axial resolution of tomograms, while the latter leads to a regular coherence function with a single central peak without a pedestal, which provides high-sensitivity image recording.

E.V. Andreeva, S.N. Il'chenko, K.M. Pankratov, V.R. Shidlovskii
Opton LLC, ul. Mosfil'movskaya 17b, 119330 Moscow, Russia;
M.A. Ladugin, A.A. Marmalyuk Sigm Plyus Ltd, ul. Vvedenskogo 3,
117342 Moscow, Russia;
S.D. Yakubovich Moscow Technological University (MIREA),
prosp. Vernadskogo 78, 119454 Moscow, Russia;
e-mail: yakubovich@superlumdiodes.com

Received 5 June 2019
Kvantovaya Elektronika 49 (10) 931–935 (2019)
Translated by M.N. Basieva

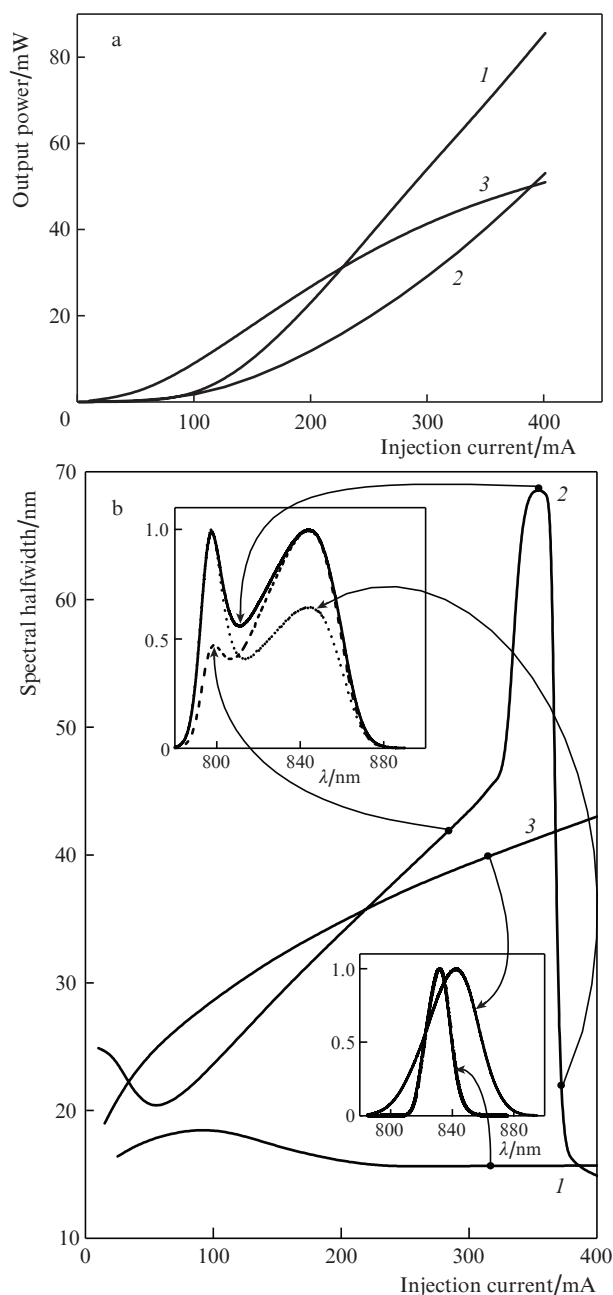


Figure 1. (a) Typical light–current characteristics and (b) dependences of the spectral halfwidth on the injection current for (1) ‘bulk’ and (2, 3) quantum-well SLDs with identical active channel configurations ($1200 \times 4 \times 0.24 \mu\text{m}$) and the active channel thicknesses of (1) 28, (2) 8.5, and (3) 6.0 nm. The insets show the SLD spectra at different injection currents.

The first-generation SLDs were based on (GaAl)As/GaAs separate-confinement double-heterostructure (SC DH) with a 'bulk' active layer about 200 nm thick (see, for example, [1, 2]). The shape of their superluminescence spectrum, which is determined by the spontaneous emission and optical gain spectra, was close to Gaussian and only slightly depended on the pump level. At active channel lengths L_a of about 1000 μm and output powers of a few and tens of milliwatts, halfwidth $\Delta\lambda$ did not exceed 20 nm.

The use of heterostructures with quantum-well active layers (nanostructures) made it possible to considerably broaden SLD spectra. The superluminescence spectrum of symmetric nanostructures with one (SQW), two (DQW), or several (MDW) quantum wells about 10 nm wide is determined by quantum transitions from the ground and excited subbands. The spectral shape strongly depends on the pump level, while the maximum spectral width is determined by the well width (energy gap between subbands) [3–5] and, under certain conditions, may exceed 100 nm [6]. The spectrum is usually double-humped-shaped, and the coherence function has a rather high pedestal.

At reasonable pump levels, SLDs based on SQW structures with an ultrathin (a few of nanometers) active layer exhibit quantum transitions only from the ground subband. The spectrum has a quasi-Gaussian profile, and the spectral width strongly depends on the length L_a and injection current (output optical power) [7]. The spectral width $\Delta\lambda$ of SLDs with $L_a > 1300 \mu\text{m}$ at free-space output power $P_{\text{FS}} > 50 \text{ mW}$ does not exceed 30–40 nm, while P_{FS} of 'short' SLDs ($L_a < 700 \mu\text{m}$) does not exceed 10 mW, but, instead, $\Delta\lambda$ may be larger than 60 nm. Figure 1 illustrates the mentioned features. This figure presents the typical light–current characteristics and the dependences of $\Delta\lambda$ on the injection current for three SLDs of identical configurations based on SC DHs differing only by the active layer thickness.

In the present work, we study experimental SLD samples based on nanostructures with two ultrathin active layers of different compositions. In this case, the superluminescence spectral width is determined by the distance between the optical gain peaks corresponding to the quantum transitions from the ground subbands of each quantum well.

2. Structure of experimental samples

The studied SLDs were based on $(\text{Al}_x\text{Ga}_{1-x})\text{As}/\text{GaAs}$ separate-confinement asymmetric DQW (ADQW) heterostruc-

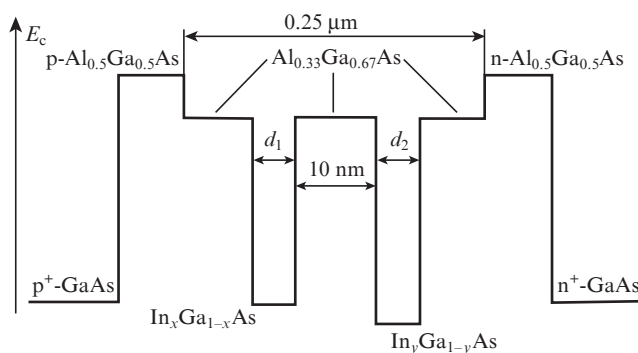


Figure 2. Band diagram of an asymmetric SC DQW structure with two quantum-well layers with thicknesses d_1 and d_2 .

Table 1. Thicknesses, compositions, and peak positions of electroluminescence spectra of the active layers of ADQW structures (type I is a symmetric DQW structure).

Structure type	d_1/nm	Composition 1	d_2/nm	Composition 2	Peak wavelengths/nm ($T = 25^\circ\text{C}$)
I	7.0	GaAs	7.0	GaAs	831
II	5.5	$\text{In}_{0.05}\text{Ga}_{0.95}\text{As}$	5.5	$\text{In}_{0.09}\text{Ga}_{0.91}\text{As}$	850, 870
III	6.5	GaAs	5.5	$\text{In}_{0.09}\text{Ga}_{0.91}\text{As}$	829, 869
IV	5.5	GaAs	5.5	$\text{In}_{0.09}\text{Ga}_{0.91}\text{As}$	816, 871
V	5.0	GaAs	5.5	$\text{In}_{0.09}\text{Ga}_{0.91}\text{As}$	808, 868

tures with two asymmetric GaAs and $(\text{In}_x\text{Ga}_{1-x})\text{As}$ active layers several nanometers thick separated by a 10-nm barrier layer. The band diagram of these heterostructures is schematically shown in Fig. 2. It should be emphasised that all the heterostructures had identical contact, emitter, and waveguide layers and differed only by thicknesses d_1 and d_2 and by the chemical compositions of active layers. These differences are demonstrated in Table 1. This table also presents the wavelengths corresponding to the electroluminescence maxima.

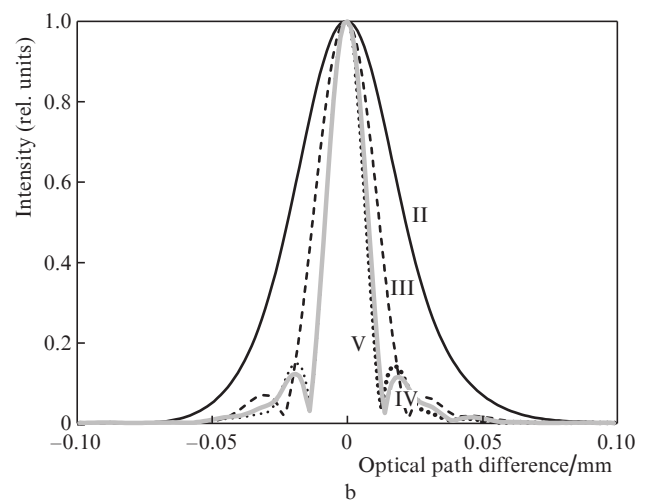
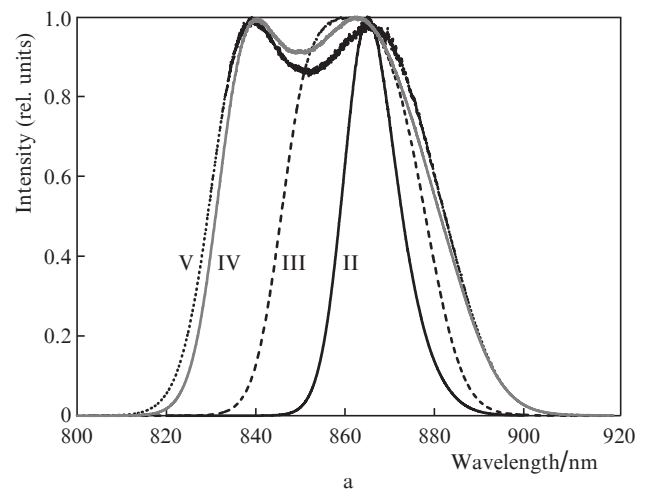


Figure 3. (a) Typical equalised spectra of SLDs of types II–V with active channel length $L_a = 1600 \mu\text{m}$ and (b) corresponding coherence functions.

Table 2. Spectral and power characteristics of SLDs of types II–V at the maximum width of the output spectrum.

Structure type	$L_a/\mu\text{m}$	λ_m/nm	$\Delta\lambda_{\text{max}}/\text{nm}$	$S_f(\%)$	I_{max}/mA	$\Delta I/\text{mA}$	$P_{\text{FS}}(I_{\text{max}})/\text{mW}$
II	1000	872	20	0	30	15	0.1
	1300	873	19	0	40	20	0.2
	1600	874	18	0	50	25	0.6
III	1000	860	36	0	60	30	2
	1300	860	35	0	90	70	8
	1600	862	33	0	130	170	17
IV	1000	857	51	12	100	35	4
	1300	858	50	10	170	70	25
	1600	859	50	8	400	150	85
V	1000	855	56	15	130	40	6
	1300	856	52	13	240	80	45
	1600	857	50	12	520	190	125

Note: λ_m is the median wavelength; $\Delta\lambda_{\text{max}}$ is the maximum halfwidth of the spectrum; S_f is the dip depth between spectral maxima; I_{max} is the injection current corresponding to $\Delta\lambda_{\text{max}}$; ΔI is the range of the injection current I , in which $\Delta\lambda > 90\% \Delta\lambda_{\text{max}}$; and P_{FS} is the output optical power.

We used a traditional SLD structure with a straight ridge active waveguide $4\ \mu\text{m}$ wide inclined at 7° with respect to the normal to the crystal faces. The waveguide length L_a was variable from 100 to $1600\ \mu\text{m}$ with a step of $100\ \mu\text{m}$. The crystal faces were coated with two-layer $\text{Al}_2\text{O}_3/\text{ZrO}_2$ antireflection films.

3. Main characteristics of studied SLDs

The change in the spectral shape of the studied SLDs with increasing injection current is qualitatively similar to that for SQW SLDs with a rather wide quantum well, in which quantum transitions may occur from the ground and excited

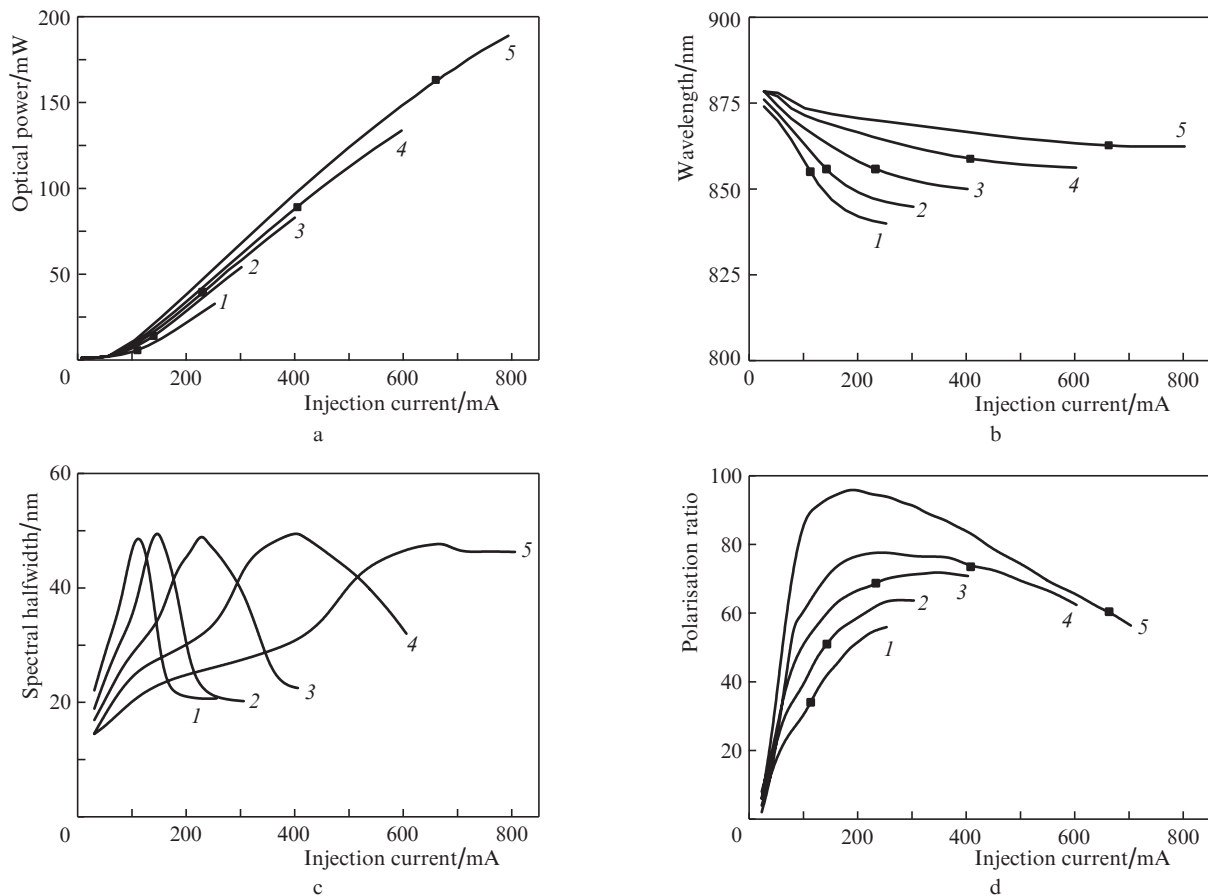


Figure 4. Dependences of (a) the output optical power P_{FS} , (b) median superluminescence wavelength λ_m , (c) spectral halfwidth $\Delta\lambda$, and (d) polarisation ratio TE/TM on the injection current at $T = 25^\circ\text{C}$ for SLD samples of type IV with active channel lengths $L_a = (1)$ 1000, (2) 1200, (3) 1400, (4) 1600, and (5) $1800\ \mu\text{m}$. The points correspond to $\Delta\lambda_{\text{max}}$.

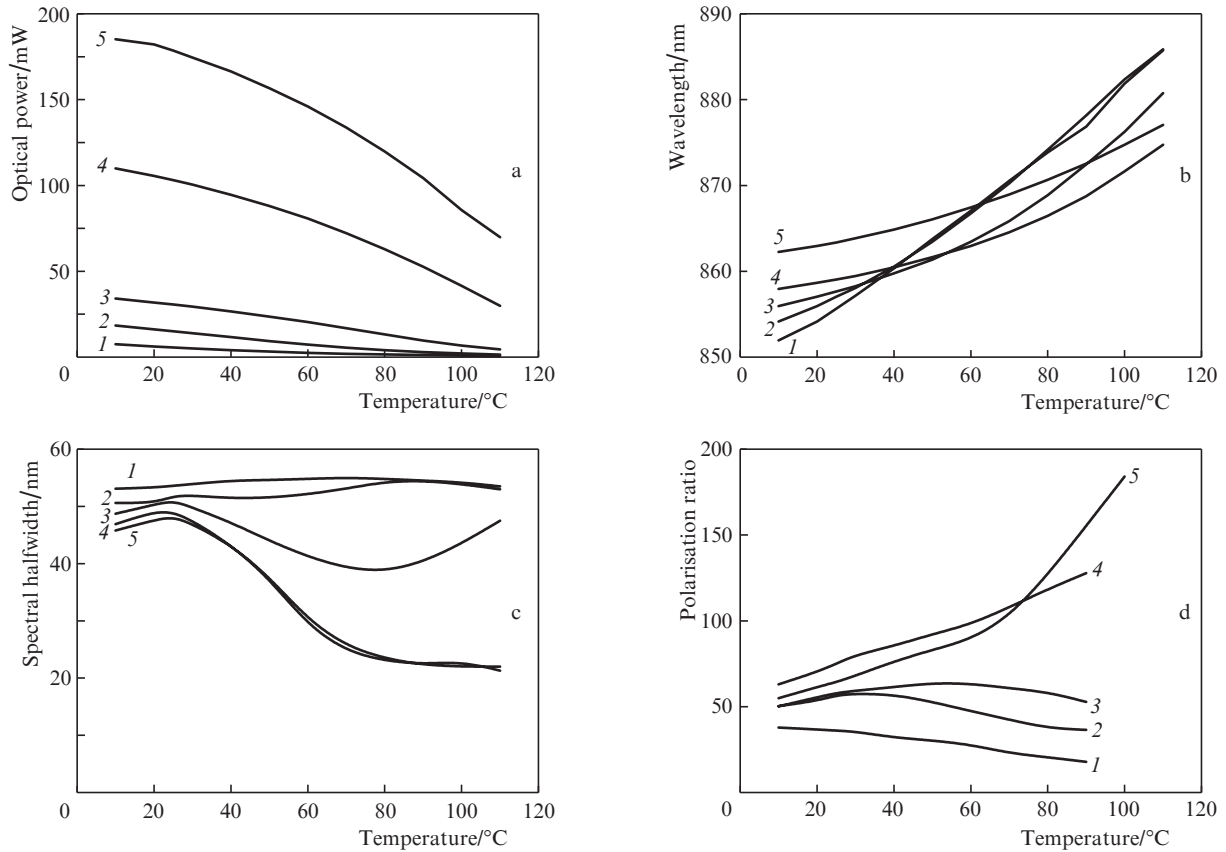


Figure 5. Dependences of (a) P_{FS} , (b) λ_m , (c) $\Delta\lambda$, and (d) TE/TM ratio on the working temperature T for SLDs of type IV with $L_a = (1)$ 1000, (2) 1200, (3) 1400, (4) 1600, and (5) 1800 μm at injection currents corresponding to $\Delta\lambda_{\text{max}}$ at $T = 25^\circ\text{C}$.

energy subbands [curve (2) in Fig. 1b]. This role in the considered ADQW structures is played by the ground states in each of the wells. An increase in the concentration of non-equilibrium charge carriers at first leads to superluminescence corresponding to stimulated transitions in the low-energy well. With increasing injection current, the spectrum broadens due to the appearance of superluminescence in the second well. At a particular current, the spectral width reaches a maximum value (Fig. 3) and then, with further increase in the current, begins to decrease because transitions in the high-energy well begin to dominate. The dependence of the spectral width on the pump level is much slower than for aforementioned SQW SLDs. The output optical power emitted at the maximum spectral width strongly depends on both the nanostructure asymmetry and the active channel length L_a . These dependences are illustrated in Table 2.

It should be noted that the width of the superluminescence spectrum of SLDs based on symmetric DQW structures with narrow quantum wells (for example, type I in Table 1) very slightly depends on current. The halfwidth of the spectrum does not exceed 18 nm at $L_a = 1000 \mu\text{m}$ and 12 nm at $L_a = 1600 \mu\text{m}$.

Of most practical interest for, first of all, light sources used in OCT systems, are SLDs of type IV (Fig. 4). Varying their active channel length, one can in a wide range (from unity to hundred milliwatts) change the output optical power at a rather wide emission spectrum ($\Delta\lambda_{\text{max}} \sim 50 \text{ nm}$) and a moderate injection current density. The studied diodes have the following advantages compared to the widely used broadband SLDs based on SQW structures with similar $\Delta\lambda_{\text{max}}$:

(i) a symmetric emission spectrum with a small depth of the spectral dip between the maxima, which by 2–3 times decreases the height of the coherence function pedestal and thus increases the sensitivity of interference measurements;

(ii) a weak dependence $\Delta\lambda(I)$: ΔI is 5–6 times larger, which considerably simplifies development of combined light sources based on two and more similar SLDs with shifted spectra;

(iii) a higher polarisation degree (the TE/TM polarisation ratio is approximately an order of magnitude higher), which

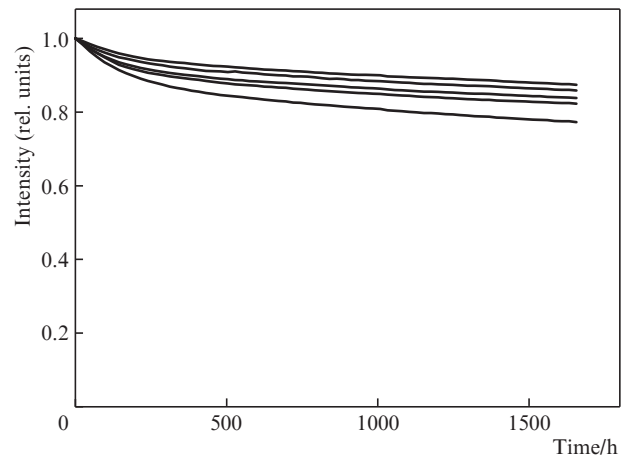


Figure 6. Chronograms of lifetime tests at $T = 25^\circ\text{C}$ for SLDs of type IV with $L_a = 1600 \mu\text{m}$ at injection current $I = 400 \text{ mA}$.

in some applications makes it possible to avoid the use of external polarisers; and

(iv) a weaker temperature dependence of the spectral width.

Figure 5 presents the temperature dependences of the main physical characteristics of the studied SLDs. These dependences unambiguously indicate that most applications require thermal stabilisation of active elements.

Preliminary lifetime tests for 2500 h at room temperature (Fig. 6) demonstrated a rather high reliability of diodes of type IV. Their estimated service time exceeds 12000 h.

4. Conclusions

It is experimentally shown that the spatially single-mode SLDs based on semiconductor ADQW structures with the optimal energy gap between the main subbands of thin quantum wells at particular injection currents have a rather broad (about 50 nm) approximately Gaussian bell-shaped emission spectrum. The output optical power of these diodes can be changed within a wide range by changing the active channel length. Compared to the widely used broadband SLDs based on SQW structures, the considered diodes have some advantages, namely, a symmetric approximately Gaussian emission spectrum, weaker dependences of the spectral width on the injection current and temperature, and a higher polarisation degree of radiation.

References

1. Kwong N.S.K., Lau K.Y., Bar-Chaim N. *IEEE J. Quantum Electron.*, **QE-25** (4), 696 (1989).
2. Safin S.A., Semenov A.T., Shidlovski V.R., Zhuchkov N.A., Kurnyavko Yu.V. *Electron. Lett.*, **28** (2) 127 (1992).
3. Batovrin V.K., Garmash I.A., Gelikonov V.M., Gelikonov G.V., Lyubarskii A.V., Plyavenek A.G., Safin S.A., Semenov A.T., Shidlovskii V.R., Yakubovich S.D. *Quantum Electron.*, **26** (2), 109 (1996) [*Kvantovaya Elektron.*, **23** (2), 113 (1996)].
4. Mamedov D.S., Prokhorov V.V., Yakubovich S.D. *Quantum Electron.*, **33** (6), 471 (2003) [*Kvantovaya Elektron.*, **33** (6), 471 (2003)].
5. Lapin P.I., Mamedov D.S., Marmalyuk A.A., Yakubovich S.D. *Quantum Electron.*, **36** (4), 315 (2006) [*Kvantovaya Elektron.*, **36** (4), 315 (2006)].
6. Il'chenko S.N., Ladugin M.A., Marmalyuk A.A., Yakubovich S.D. *Quantum Electron.*, **42** (11), 961 (2012) [*Kvantovaya Elektron.*, **42** (11), 961 (2012)].
7. Andreeva E.V., Il'chenko S.N., Kostin Yu.O., Ladugin M.A., Lapin P.I., Marmalyuk A.A., Yakubovich S.D. *Quantum Electron.*, **43** (8), 751 (2013) [*Kvantovaya Elektron.*, **43** (8), 751 (2013)].